Role of interface quality in vortex pinning by large nonsuperconducting particles

N. Adamopoulos and S. K. Patapis
Section of Solid State Physics, Department of Physics, University of Athens, Panepistimiopolis, GR 157 84 Athens, Greece
(Received 24 May 1999)

It is widely believed that large nonsuperconducting particles inhibit the flow of the electric current and result in lower critical current density due to the reduction of the cross sectional area. However, it will be shown that the spatial variation of the magnetic penetration depth can lead to pinning of the vortices and increased critical current density provided that the interface between the superconducting phase and the nonsuperconducting particles is sharp.

It is known that the magnetic interaction can be a source of pinning and the resulting pinning force can contribute significantly to the overall volume pinning force. Y-123 materials containing 211 particles[1] as well as Bi-2212 materials containing MgO whiskers[2] are two of the examples where the effect of the magnetic pinning mechanism has been demonstrated in numerous experiments. In order, however, for such a pinning mechanism to be effective the interface between the superconducting matrix and the nonsuperconducting particles has to be sharp. The interaction of the magnetic field of a vortex in the vicinity of the normal phase particle with the normal phase causes a reduction of the magnetic energy of the vortex and creates a pinning site acting an attractive force to the vortex. This effect can lead to high values of the pinning force in cases where the second nonsuperconducting particles have been added at the initial stage of the preparation of the material, or have been tailored through the heat treatment process. It can also take place in cases where the second particles are created unintentionally and are considered to prohibit the smooth flow of the supercurrent, as in the case of 2201 particles in Bi-based materials:[3] at temperatures where the 2201 phase is normal the pinning effect is strong, an effect which compensates partially the loss of a part of the superconducting cross sectional area.

The magnetic pinning interaction with large planar defects will be studied for the case of a gradual variation of the properties of the material from the superconducting matrix to the normal phase of the defect. This situation reflects the microstructure in real materials; it has been shown for example that the interface between the host superconductor and the MgO whiskers in Bi-2212 composite reaction textured materials is sharp of the order of a few atomic spacings.[2] In the above case it was demonstrated that the introduction of MgO whiskers increases the pinning force and the critical current density up to a volume fraction of about 35%.

The analysis is based on the modified second London equation and it shows that in order for the magnetic pinning mechanism to contribute significantly to the overall pinning force the interface of the matrix and the defect must be sharp.

Pinning of a flux line by an interface between two superconductors has been studied in the past,[4] here, however, we attempt to study the case not of a sharp interface, but of a gradual suppression of the superconducting properties. Our approach is triggered by the observation of real materials and interfaces as they appear in a high-resolution electron microscope, where it can be seen that seldom the interface between a superconductor and normal particle is sharp,[2,3] and very often the interface extends to several unit cells before the crystal structure of each phase is reestablished.

It must also be pointed out that our model is one-dimensional. The flux line is modeled as a magnetic field which varies only along the x direction. This, however, is not the common practice. A full description of a flux line is that of the fluxoid with a delta function with an y as well an x component. The model presented here can not be considered as a full treatment of problem; on the other hand it provides invaluable qualitative information of the bulk pinning force one should expect in a material with a given microstructure. In addition, the applicability of the model can be tested in the extreme limits where the results for a flux line pinned by a sharp interface are known.

The geometry of the model used in the present analysis is as shown in Fig. 1: a planar defect of penetration depth λ_2 is introduced in a superconducting matrix of penetration depth λ_1, with $\lambda_2 > \lambda_1$. The interface has a spatial extension D, and a vortex is pointing in the z direction and is positioned at $\mathbf{r}_0$. The modified second London equation is given as[5]

$$\mathbf{B} + \nabla \times (\lambda^2 \nabla \times \mathbf{B}) = \Phi_0 \delta(\mathbf{r} - \mathbf{r}_0)\hat{e}_z . \tag{1}$$

For a simple one-dimensional model where the magnetic penetration depth $\lambda(x)$ varies along the axis $\hat{x}$, the above equation reduces to

$$-\lambda^2(x)\frac{\partial^2 B}{\partial x^2} - 2\lambda(x)\frac{\partial \lambda}{\partial x}\frac{\partial B}{\partial x} + B(x) = \Phi_0 \delta(x - x_0). \tag{2}$$

A linear variation of the penetration depth across the interface has been used, as depicted in Fig. 1. The penetration length in region II is described as $\lambda(x) = \lambda_2 + [(\lambda_1 - \lambda_2)/D]x$ or $\lambda(x) = \lambda_2 + Ax$ for $A = (\lambda_1 - \lambda_2)/D$. In regions I and III the penetration depth is constant and equal to λ_1 and λ_2, respectively. If the flux line is positioned in region I at position x_0, Eq. (2) becomes

$$\text{region I:}\quad \frac{\partial^2 B}{\partial x^2} - \frac{1}{\lambda_1^2} B = -\frac{\Phi_0}{\lambda_1^2}\delta(x - x_0), \tag{3a}$$

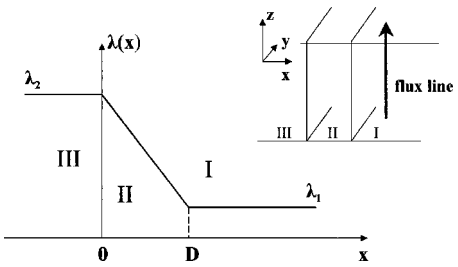

FIG. 1. Variation of the penetration depth across the interface between the superconducting matrix and a nonsuperconducting particle. The normal phase is occupying the space $x<0$, while the space $0<x<D$ denotes the gradual suppression of the superconducting properties. A linear reduction of the penetration length as shown in the figure has been used for the present model. This model is the one-dimensional analogue of the three-dimensional problem the geometry of which is schematically drawn in the upper part of the figure.

$$\text{region II:}\quad \frac{\partial^2 B}{\partial x^2}+\frac{2A}{\lambda_2+Ax}\frac{\partial B}{\partial x}-\frac{1}{(\lambda_2+Ax)^2}B=0, \tag{3b}$$

$$\text{region III:}\quad \frac{\partial^2 B}{\partial x^2}-\frac{1}{\lambda_2^2}B=0. \tag{3c}$$

The solution to above equations is presented in the Appendix A, and is summarized as follows.

$$\text{Region I:}\quad B_{\mathrm{I}}(x)=A_1 e^{-x/\lambda_1}+A_2 e^{-|x-x_0|/\lambda_1}, \tag{4a}$$

$$\text{region II:}\quad B_{\mathrm{II}}(x)=[1/(\lambda_2+Ax)]\times[C_1(\lambda_2+Ax)^{s_1}+C_2(\lambda_2+Ax)^{s_2}], \tag{4b}$$

$$\text{region II:}\quad B_{\mathrm{III}}(x)=D_1 e^{x/\lambda_2}. \tag{4c}$$

The unknown constants A_1, C_1, C_2, and D_1 can be evalu ated through the condition that at the boundaries between the three regions of the model the magnetic field and its derivative must be continuous:

$$B_{\mathrm{I}}(D)=B_{\mathrm{II}}(D),\quad B'_{\mathrm{I}}(D)=B'_{\mathrm{II}}(D)$$

$$B_{\mathrm{II}}(0)=B_{\mathrm{III}}(0),\quad B'_{\mathrm{II}}(0)=B'_{\mathrm{III}}(0). \tag{5}$$

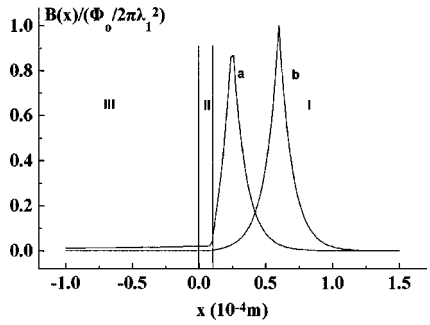

FIG. 2. Plot of the magnetic field around a vortex positioned close (a) and away from the defect (b). The presence of the interface distorts the magnetic field. $\lambda_1=10^{-4}$ m, $\lambda_2=20\lambda_1$, $D=\lambda_1$, $x_0=2.5\lambda_1$ (a), $x_0=6\lambda_1$ (b).

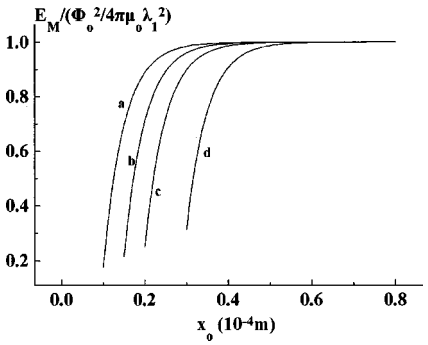

FIG. 3. Plot of the magnetic energy per unit length of a vortex as a function of the distance from the defect boundary at $x=D$, for $\lambda_1=10^{-4}$ m, $\lambda_2=20\lambda_1$, $D=\lambda_1$ (case a), $D=1.5\lambda_1$ (case b), $D=2\lambda_1$ (case c), and $D=3\lambda_1$ (case d).

The above equations are a direct result of the condition that at the boundary between two superconductors the normal component of the magnetic field and the tangential component of $\lambda^2\mathbf{J}$ are continuous (Ref. 6).

The solution of Eq. (5) is presented in Appendix B. The magnetic field around a vortex can then be deduced from the present model and is plotted in Fig. 2 for $\lambda_2=20\lambda_1$, $D=\lambda_1$, $x_0=2.5\lambda_1$, and for $x_0=6\lambda_1$, from it is shown that the presence of the interface strongly distorts the magnetic field.

The magnetic energy per unit length is calculated as $E_M=(1/2\mu_0)\Phi_0 B(x_0)$ (Ref. 5) and is plotted in Fig. 3 as a function of the distance from the interface x_0, and for different values of the parameter D. The pinning force per unit length is calculated as $f=-\partial E_M/\partial x_0$ and is plotted in Fig. 4 for several values of the ratio λ_2/λ_1 and as a function of the sharpness of the interface as this is characterized by the ratio D/λ_1. It is clear from Fig. 4 that a sharp interface having a low value of D/λ_1 produces a strong pinning force, and this pinning force is getting higher for large values of the ratio λ_2/λ_1. It can be seen that the maximum pinning force per unit length is produced when $\lambda_2\gg\lambda_1$ and $D\ll\lambda_1$, and it takes the value of (see Appendix B):

$$F_{\max}=\Phi_0^2/2\pi\mu_0\lambda_1^3 \tag{6}$$

while the pinning force per unit length as a function of the distance from the interface is expressed as

$$f(x_0)=-(\Phi_0^2/2\pi\mu_0\lambda_1^3)e^{-2(D-x_0)/\lambda_1}. \tag{7}$$

Equation (7) may be compared with the exact result of the pinning force per unit length[6] in the vicinity of a free surface $f(x_0)=-(\Phi_0^2/2\pi\mu_0\lambda_1^3)K_1(2x_0/\lambda_1)$, where K_1 is the modified Bessel function, from which it can be concluded the very good qualitative and quantitative agreement of the present model with the pinning of a flux line by a free surface in the limit $\lambda_2\gg\lambda_1$ and $D\ll\lambda_1$.

An important conclusion that can be drawn from the present model is the dependence of the maximum pinning force on the degree of change of the penetration length across the interface, or in other words on the value of D/λ_1. Figure 4 shows this dependence for five values of the ratio λ_2/λ_1 as a function of the distance from the interface. The higher this ratio, the stronger is the maximum pinning force and the weaker is its dependence on the distance from the

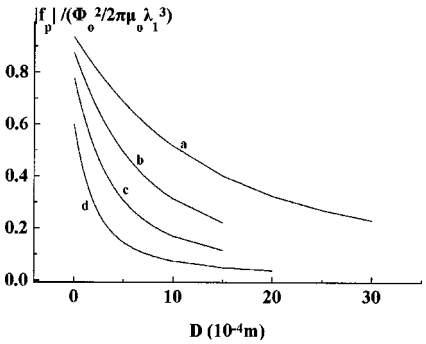

FIG. 4. Absolute value of the maximum pinning force as a function of interface sharpness. $\lambda_1 = 0.5 \times 10^{-4}$ m, $\lambda_2 = 30\lambda_1$ (case a), $\lambda_2 = 15\lambda_1$ (case b), $\lambda_2 = 8\lambda_1$ (case c), $\lambda_2 = 4\lambda_1$ (case d).

interface. This confirms that sharp interfaces exert strong pinning forces, and these pinning forces have a long range of action.

Considering now the case of the Bi-2223 material for which it has been shown that the 2223 phase coexists with the 2212, we can estimate from the present model the pinning well which forms in the boundary between the two phases. Taking the penetration length at 0 K λ_0 to be 250 nm, we can estimate the penetration depth for each phase at 77 K through the relation $\lambda(T) = \lambda_0 / \sqrt{1-(T/T_c)^4}$. The maximum pinning force for an interface where $D = 0$ can be derived from the present model and it can be shown that it takes the value of Eq. (6) reduced by a factor of $(\lambda_2 - \lambda_1)/(\lambda_2 + \lambda_1)$, which factor for this case becomes 0.08. This pinning force compensates partially the loss of the most effective current-carrying 2223 phase.

Flux lines can be pinned by various mechanisms in a superconductor, and for most cases these have been classified into two broad categories, the core interaction, and the magnetic interaction.[7,8] We believe, however, that this distinction is not useful when studying pinning by large pinning centers of the order of the penetration depth as both types of pinning mechanism occur simultaneously. The pinning potential can be thought as having two characteristic geometric lengths as is shown schematically in Fig. 5: the first is the coherence length ξ over which the wave function changes dramatically, and the penetration depth λ over which the magnetic field and the surrounding supercurrents decay. If the interface is not sharp of the order of the coherence length the pinning force is getting reduced. As the coherence length in the high T_c superconductors in the direction parallel to *a,b* planes is 3–4 nm it is concluded that the interface between the host superconductor and a normal particle or void must not extend to more than a few unit cells. The contribution however to pinning potential from the magnetic field is sensitive to any distortion of the magnetic field around a vortex.

The above argument can be supported by experiments done Pb-36% Tl by varying the diffusion distance,[9] where it was shown that as the thallium was diffused into the sample the screening currents were reduced in a fashion which is in very good agreement with our results shown in Fig. 4. If one takes also into account the interaction between the flux lines, it can be concluded that the transition from normal to superconducting material must occur over a distance less than one vortex spacing a_0, and the size of the inclusions must be of the order of a_0.

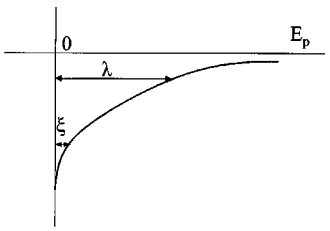

FIG. 5. Spatial variation of the pinning potential around a large pinning center.

This contribution therefore accounts for the attraction of an isolated vortex far away from the defect, as this force however is weak the pinning of the vortex is subject to its interaction with the flux line lattice and the driving force. In other words, the pinning potential due to magnetic interaction can be deep while the pinning force may be small.

The distinction, however, between the core and the magnetic pinning effect is useful when one wishes to determine the predominant pinning mechanism in the material. This can be done as the two different contributions have different field and temperature dependence. Previous experiments have demonstrated that in certain types of material the magnetic pinning is the dominant pinning mechanism. This is the case of Pb-Bi ε-phase matrix with tungsten particles.[9]

Significant contribution to the overall pinning strength in Y-123 materials has also been proved to be provided from the dispersed 211 particles,[1,10] while subsequent studies have revealed that the large 211 precipitates increase the irreversibility line[11] due to the interface with the superconducting phase. The degree of sharpness of the interface has, however, yet to be optimized to obtain the maximum available pinning force.

Another example of magnetic pinning due to an interface is the presence of twin boundaries in Y-123 materials. It is well established that the twin boundaries not only pin the flux lines, but by orienting the external magnetic field with the planar interface of a twin boundary we can also alter the whole magnetic behavior of the material.[12,13] Large planar interfaces exist in every case there exists a large precipitate or a nonsuperconducting inclusion in a superconducting host material.[9,14] The magnetic interaction provides a strong pinning but in order for such a contribution to become most effective the transition between the two phases must happen over a distance which is short comparative to the penetration length. As has been stated in the previous paragraph, MgO whiskers in Bi-2212 material provide large and sharp planar interfaces and this has been demonstrated by HREM images.[2]

In conclusion, we have calculated the pinning force resulting from the variation of the penetration depth inside a superconductor. The analysis of the linear model used to describe the mode of variation of the superconducting properties reproduces the well known result of flux line pinning by the free surface of the material. It is shown that as the interface sharpness decreases, the pinning force is reduced in agreement with previous experiments. It can be concluded that around large nonsuperconducting particles both types of pinning mechanism, the core and the magnetic interaction, are present and affect the shape of the pinning potential. It can be argued that the microstructural characteristics will

finally determine which superconducting characteristic length plays the most effective role in deriving the pinning force from the pinning potential. The present model provides a useful tool to estimate to degree of the suppression of the pinning force to be expected having in mind the microstructural state of the sample as observed in a high-resolution electron microscope.

APPENDIX A

In region I Eq. (3a) is the well-known modified second London equation for a homogeneous medium and the solution will be

$$B_I(x)=A_1e^{-x/\lambda_1}+A_2e^{-|x-x_0|/\lambda_1},$$

where the first term is the solution of the homogeneous equation and the second term is the specific solution with $A_2=\Phi_0/2\pi\lambda_1^2$.

In region II, the solution of Eq. (3b) can be simplified with the substitution $\lambda_2+Ax=\omega$, and Eq. (3b) then becomes[15]

$$\frac{\partial^2 B_{\rm II}}{\partial\omega^2}+2\frac{1}{\omega}\frac{\partial B_{\rm II}}{\partial\omega}-\frac{1}{A^2}\frac{1}{\omega^2}B_{\rm II}=0. \tag{A1}$$

Equation (A1) has the form $B_{\rm II}''+PB_{\rm II}'+QB_{\rm II}=0$, where $P=2/\omega$ and $Q=-1/(A^2\omega^2)$, and its solution will be $B_{\rm II}=e^{-(1/2)\int Pd\omega}b$, where b satisfies the equation

$$b''+(Q-P'/2-P''/4)b=0. \tag{A2}$$

Equation (A2) takes the simple form $b''-(1/A^2\omega^2)b=0$. By making the substitution $b=\omega^s$ we find that s satisfies the equation $s^2-s-(1/A^2)=0$, which has the solution $s_{1,2}=(1\pm\sqrt{1+4/A^2})/2$.

It is finally concluded that the magnetic field in region II has the form

$$B_{\rm II}(x)=\frac{1}{\lambda_2+Ax}[C_1(\lambda_2+Ax)^{s_1}+C_2(\lambda_2+Ax)^{s_2}].$$

In region III, Eq. (3c) is the second London equation for a medium of penetration depth λ_2 and its solution is

$$B_{\rm III}(x)=D_1e^{x/\lambda_2}.$$

APPENDIX B

The constants A_1,C_1,C_2,D_1 of Eq. (5) are the solutions of the following system of equations in a matrix form

$$\begin{bmatrix}A_1\\C_1\\C_2\\D_1\end{bmatrix}=\begin{bmatrix}e^{-D/\lambda_1} & -\lambda_1^{s_1-1} & -\lambda_1^{s_2-1} & 0\\ 0 & \lambda_2^{s_1-1} & \lambda_2^{s_2-1} & -1\\ -e^{-D/\lambda_1} & -A(s_1-1)\lambda_1^{s_1-1} & -A(s_2-1)\lambda_1^{s_2-1} & 0\\ 0 & A(s_1-1)\lambda_2^{s_1-1} & A(s_2-1)\lambda_2^{s_2-1} & -1\end{bmatrix}^{-1}\begin{bmatrix}-A_2e^{-(D-x_0)/\lambda_1}\\0\\-A_2e^{-(D-x_0)/\lambda_1}\\0\end{bmatrix}. \tag{B1}$$

The solution to the above matrix equation is straightforward. The results, however, are very lengthy, and we shall give below only the results for the limit of $\lambda_2\gg\lambda_1$ where $s_1\to1$ and $s_2\to0$:

$$A_1=-A_2e^{(D-x_0)/\lambda_1}e^{D/\lambda_1}\frac{A\lambda_2-\lambda_1-A\lambda_1-\lambda_2}{A\lambda_2+\lambda_1+A\lambda_1+\lambda_2}, \tag{B2}$$

$$C_1=2A_2e^{(D-x_0)/\lambda_1}\frac{\lambda_1}{\lambda_2+\lambda_1}, \tag{B3}$$

$$C_2=-2A_2e^{(D-x_0)/\lambda_1}\frac{\lambda_1\lambda_2}{A\lambda_2+\lambda_1+A\lambda_1+\lambda_2}, \tag{B4}$$

$$D_1=2A_2e^{(D-x_0)/\lambda_1}\frac{\lambda_1A}{A\lambda_2+\lambda_1+A\lambda_1+\lambda_2}. \tag{B5}$$

[1] M. Murakami *et al.*, Cryogenics **32**, 930 (1992).
[2] N. Adamopoulos *et al.*, Physica C **242**, 68 (1995).
[3] Y. Yan *et al.*, Appl. Phys. Lett. **67**, 2554 (1995).
[4] G. S. Mkrtchyan *et al.*, Zh. Eksp. Teor. Fiz. **63**, 667 (1972) [Sov. Phys. JETP **36**, 352 (1973)].
[5] M. Tinkham, *Introduction to Superconductivity* (McGraw-Hill, New York, 1975).
[6] T. P. Orlando and K. Delin, *Foundations of Applied Superconductivity* (Addison-Wesley, New York, 1991).
[7] H. Ullmaier, *Irreversible Properties of Type II Superconductors* (Springer-Verlag, Berlin, 1975).
[8] E. H. Brandt, Rep. Prog. Phys. **58**, 1465 (1995).
[9] A. M. Campbell and J. E. Evetts, Adv. Phys. **21**, 199 (1972).
[10] K. Kimura *et al.*, *Critical Currents In Superconductors* (World Scientific, Singapore, 1994), p. 415.
[11] M. Watahiki *et al.*, Physica C **296**, 43 (1998).
[12] H. Pastoriza *et al.*, Phys. Rev. B **83**, 1026 (1999).
[13] C. Reichhardt, C. J. Olson, and F. Nori (unpublished).
[14] T. Matsushita, Jpn. J. Appl. Phys. **20**, 1153 (1981).
[15] X. G. Qiu *et al.*, Physica C **216**, 49 (1993).